A Modified Method of Approximate Particular Solutions for Solving Linear and Nonlinear PDEs

Guangming Yao,[1] **Ching-Shyang Chen**,[2] **Hui Zheng**[3]
[1] *Department of Mathematics, Clarkson University, Potsdam, New York 13699-5815*

[2] *Department of Mathematics, University of Southern Mississippi, Hattiesburg, Mississippi 39406-5045*

[3] *Department of Civil Engineering, Nanchang University, China*

Received 14 August 2015; revised 27 February 2017; accepted 1 March 2017
Published online in Wiley Online Library (wileyonlinelibrary.com).
DOI 10.1002/num.22161

The method of approximate particular solutions (MAPS) was first proposed by Chen et al. in Chen, Fan, and Wen, Numer Methods Partial Differential Equations, 28 (2012), 506–522. using multiquadric (MQ) and inverse multiquadric radial basis functions (RBFs). Since then, the closed form particular solutions for many commonly used RBFs and differential operators have been derived. As a result, MAPS was extended to Matérn and Gaussian RBFs. Polyharmonic splines (PS) has rarely been used in MAPS due to its conditional positive definiteness and low accuracy. One advantage of PS is that there is no shape parameter to be taken care of. In this article, MAPS is modified so PS can be used more effectively. In the original MAPS, integrated RBFs, so called particular solutions, are used. An additional integrated polynomial basis is added when PS is used. In the modified MAPS, an additional polynomial basis is directly added to the integrated RBFs without integration. The results from the modified MAPS with PS can be improved by increasing the order of PS to a certain degree or by increasing the number of collocation points. A polynomial of degree 15 or less appeared to be working well in most of our examples. Other RBFs such as MQ can be utilized in the modified MAPS as well. The performance of the proposed method is tested on a number of examples including linear and nonlinear problems in 2D and 3D. We demonstrate that the modified MAPS with PS is, in general, more accurate than other RBFs for solving general elliptic equations. Numer Methods Partial Differential Eq 000: 000–000, 2017

Keywords: MAPS; polyharmonic splines; multiquadric; variable coefficient PDEs; radial basis functions

I. INTRODUCTION

During the last decade, radial basis functions (RBFs) [1–5] have been broadly applied for solving various kinds of partial differential equations (PDEs). A RBF, $\phi_j(\mathbf{x})$ is a function that depends only on the distance to a center point $\mathbf{x}_j$. Thus, it can be rewritten as $\phi_j(\mathbf{x}) = \phi(\|\mathbf{x}-\mathbf{x}_j\|) = \phi(r)$,

Correspondence to: Guangming Yao, Department of Mathematics, Clarkson University, Potsdam, NY 13699-5815 (e-mail: gyao@clarkson.edu)

TABLE I. List of commonly used RBFs.

Name of RBFs	Formulation
Gaussian (GA)	$\phi(r) = \exp\left(-cr^2\right), \quad c > 0$
Multiquadric (MQ)	$\phi(r) = \sqrt{r^2 + c^2}, \quad c > 0$
Inverse multiquadric (IMQ)	$\phi(r) = 1/\sqrt{r^2 + c^2}, \quad c > 0$
Matérn of order m	$\phi(r) = \begin{cases} (cr)^m K_m(cr), & r > 0 \\ m\Gamma(m), & r = 0 \end{cases}$
Polyharmonic splines (PS) of order m	$\phi(r) = r^{2m} \ln(r),$ $\phi(r) = r^{2m-1}$

where $r = \|\mathbf{x} - \mathbf{x}_j\|$. This notation indicates the numerical procedure involving RBFs in high-dimensional space will be the same as for problems in one-dimensional space, except that the distance needs to be redefined. The RBFs may also have a shape parameter c, in which case $\phi(r)$ can be replaced with $\phi(r, c)$. Some of the commonly used RBFs are given in Table I, in which all but polyharmonic splines (PS) have shape parameters. Multiquadric (MQ) is one of the most commonly used RBFs.

One category of the methods that use RBFs to solve PDEs is the collocation method. The RBF collocation method discretizes PDEs into a system of algebraic equations. There is no mesh or integration needed in the discretization process. The only information we need is the discretized data points and the distance between pairwise points. Distances are easy to compute in any number of space dimensions, so working on higher-dimensional problems using the RBF collocation method does not increase the difficulty. One of the attractions of RBF collocation methods for solving PDEs is the simplicity. It is flexible with respect to the geometry of the domain and is computationally efficient.

Among all of the collocation methods, the collocation process can be done in two different ways. Traditionally, an RBF expansion is introduced with unknown coefficients for the solution to the PDE, then differentiated and collocated. We call it the direct RBF collocation method. On the other hand, indirect RBF collocation can be done by integration instead of differentiation. The method of approximate particular solutions (MAPS) [6–8], is a collocation method that is a recently developed indirect RBF collocation method. In MAPS, the experimental data (inhomogeneous term) are interpolated by RBFs, then integrated in the polar coordinate system and collocated strictly on the governing equation and boundary conditions. It is slightly more accurate compared to the direct RBF collocation techniques. MAPS has been extended to many RBFs including Gaussian, MQ, IMQ, and Matérn RBFs [9–11]. These RBFs all contain shape parameters and are infinitely smooth.

In addition, when RBFs containing the shape parameters are used, we can usually justify the shape parameter to find an optimal approximation to the solutions to PDEs without increasing the size of the data samples. However, finding an optimal shape parameter can be a challenge [12–18]. PS [19, 20], conversely, does not contain a shape parameter. In the past, PS was not seriously considered in the implementation for solving PDEs due to its low convergence. Another difficulty is the handling of the augmented polynomial terms for high-order PS which is quite tedious. As a result, PS has not been fully explored in the area of RBF collocation methods.

In this article, we investigate and discover the impact of these additional augmented polynomials on the accuracy when the order of PS is sufficiently large. As we shall see in many of our numerical examples, the accuracy continues to move up when the order of PS goes higher (up to order 15 in all examples but Example 2). In Example 2, which is a Poisson problem involving Runge function, MAPS with PS works slightly better than with MQ when polynomials of degree 2 to 4 are used.

One of the advantages of the shape parameter of MQ is that one can increase the accuracy by adjusting the shape parameter properly without additional cost. However, finding a good shape parameter can be challenge and time consuming. Furthermore, numerical experiments suggest that PS is more attractive compared to MQ in general in MAPS, since we do not need to handle the shape parameter in PS and we do not gain accuracy when we use MQ. We can increase the order of PS to improve the accuracy with very little additional cost. We believe this discovery is significant to RBF collocation methods. Although the idea of adding additional polynomial basis to RBF basis are not new, emphasis of this article is the combination of the polyharmonic splines integrated in radial space with non-integrated polynomial basis leads better results than other RBFs in our experiments of linear and nonlinear PDEs.

The structure of the article is as follows. In Section II, we propose to reformulate MAPS based on PS and polynomial kernels. In Section III, five examples in 2D and 3D are given to demonstrate the effectiveness of the proposed modified MAPS using PS and MQ. A short conclusion is drawn in Section IV.

II. MAPS USING POLYHARMONIC SPLINES

In this section, MAPS using PS is presented for solving elliptic PDEs of the form

$$\mathbf{L}u(\mathbf{x}) = f(\mathbf{x}), \quad \mathbf{x} \in \Omega, \tag{1}$$

$$\mathbf{B}u(\mathbf{x}) = g(\mathbf{x}), \quad \mathbf{x} \in \partial\Omega. \tag{2}$$

where $\mathbf{L}$ and $\mathbf{B}$ are linear partial differential operators, $\Omega \subset \mathbb{R}^d, d = 2, 3$, is a bounded and closed domain with boundary $\partial\Omega$. RBF collocation methods discretize linear PDEs into a linear system of equations by collocation. The coefficient matrix in the linear system is called the collocation matrix. The interpolation matrix generated by PS RBFs can be singular, even with non-trivial sets of distinct centers [19, 20]. Typically, to insure the invertibility of the collocation system, a low-order polynomial basis has to be augmented to the RBF basis. Furthermore, the PS RBFs are called conditionally positive definite. Let $\{\mathbf{x}_i\}_{i=1}^n \in \mathbf{R}^d$, $d = 2, 3$, be all interpolation points. Let $\mathscr{P}_m^d$ be the set of d-variate polynomials of degree up to m and $\{p_l\}_{l=1}^w$ be a basis of $\mathscr{P}_m^d$ where

$$w = \binom{m+d}{d} = \begin{cases} \dfrac{1}{2}(m+2)(m+1), & \text{in } \mathbf{R}^2, \\ \dfrac{1}{6}(m+1)(m+2)(m+3), & \text{in } \mathbf{R}^3, \end{cases} \tag{3}$$

is the dimension of the polynomial space $\mathscr{P}_m^d$. MAPS can approximate the solution to (1)–(2) at a discrete set of evaluation points. For simplicity, we will introduce MAPS by approximation of the solution at the given interpolation points, $\{\mathbf{x}_i\}_{i=1}^n$. Let $\phi(r)$ be PS of degree m (see Table I), and

$\{p_l\}_{l=1}^{w}$ be the polynomial basis. In MAPS, we assume the solution to (1)–(2) can be approximated by the particular solutions and the polynomials in the following manner:

$$u(\mathbf{x}) \approx \hat{u}(\mathbf{x}) = \sum_{j=1}^{n} \alpha_j \Phi(\|\mathbf{x} - \mathbf{x}_j\|) + \sum_{l=1}^{w} \alpha_{n+l} p_l(\mathbf{x}), \tag{4}$$

where $\{\alpha_j\}$ is the undetermined coefficient, Φ is a particular solution with respect to ϕ and differential operator $\mathbf{L}$,

$$\mathbf{L}\Phi(r) = \phi(r), \tag{5}$$

and the augmented polynomial bases are shown as follows:

$$p_l(\mathbf{x}) = \begin{cases} x^{i-j}y^j, & 0 \le j \le i,\ 0 \le i \le m, \quad \text{in } \mathbf{R}^2, \\ x^{i-j-k}y^j z^k, & 0 \le k \le i-j,\ 0 \le j \le i,\ 0 \le i \le m, \quad \text{in } \mathbf{R}^3, \end{cases}$$

where m is the order of the polynomial basis as shown in (3). By direct differentiation, we obtain a set of polynomials $q_l(\mathbf{x})$ such that

$$\mathbf{L}p_l(\mathbf{x}) = q_l(\mathbf{x}), \qquad l = 1, 2, \cdots, w. \tag{6}$$

As stated in [21], the use of polynomial is somewhat arbitrary. That says any other set of w linearly independent basis functions could also be used. It is easy to see that the addition of polynomials of total degree at most m guarantees polynomial precision provided the points in the domain from an m-unisolvent set. In other words, if the data come from a polynomial of degree less than or equal to m, then they are fitted exactly by the expansion of the basics, assuming that no Runge's phenomenon arises. There are many other numerical issues while using polynomial basis. We will test the effect of the additional polynomial basis with integrated polyharmonic splines through numerical examples.

For any point $\mathbf{x} \in \Omega$, by interpolating the forcing term in (1) using the PS and polynomial kernels, we have

$$\sum_{j=1}^{n} \alpha_j \phi(\|\mathbf{x} - \mathbf{x}_j\|) + \sum_{l=1}^{w} \alpha_{n+l} q_l(\mathbf{x}) = f(\mathbf{x}). \tag{7}$$

Let the first n_i points be the interior points in Ω, and the next n_b points be the boundary points on $\partial\Omega$. The total number of collocation points is $n = n_i + n_b$. Then, by the collocation method, we have the following linear system in Ω:

$$\mathbf{L}\hat{u}(\mathbf{x}_k) = \sum_{j=1}^{n} \alpha_j \phi(\|\mathbf{x}_k - \mathbf{x}_j\|) + \sum_{l=1}^{w} \alpha_{n+l} q_l(\mathbf{x}_k) = f(\mathbf{x}_k), k = 1, 2, \ldots, n_i. \tag{8}$$

As there are w additional degrees of freedoms in (8), the standard polynomial insolvency constraint [3] must be applied

$$\sum_{j=1}^{n_i} \alpha_j q_l(\mathbf{x}_j) = 0, l = 1, 2, \ldots, w. \tag{9}$$

TABLE II. The closed form particular solutions $\Delta\Phi(r) = \phi(r)$ in $\mathbf{R}^2$.

RBF	$\phi(r)$	$\Phi(r)$
PS	$r^{2m}\ln(r)$	$\frac{r^{2m+2}\ln r}{4(m+1)^2} - \frac{r^{2m+2}}{4(m+1)^3}$
MQ	$\sqrt{r^2+c^2}$	$\frac{1}{9}\left(4c^2+r^2\right)\sqrt{r^2+c^2} - \frac{c^3}{3}\ln\left(c+\sqrt{r^2+c^2}\right)$

TABLE III. The particular solutions $\Delta\Phi(r) = \phi(r)$ in $\mathbf{R}^3$.

RBF	$\phi(r)$	$\Phi(r)$
PS	r^{2m-1}	$\frac{r^{2m+1}}{(2m+1)(2m+2)}$
MQ	$\sqrt{r^2+c^2}$	$\begin{cases} \frac{(5c^2+2r^2)\sqrt{r^2+c^2}}{24} + \frac{c^4}{8r}\ln\left(\frac{r+\sqrt{r^2+c^2}}{c}\right), & r \neq 0 \\ \frac{c^3}{3}, & r = 0 \end{cases}$

Similarly, on the boundary $\partial\Omega$, we have

$$\mathbf{B}\hat{u}(\mathbf{x}_k) = \sum_{j=1}^{n} \alpha_j \mathbf{B}\Phi(\|\mathbf{x}_k - \mathbf{x}_j\|) + \sum_{l=1}^{w} \alpha_{n+l}\mathbf{B}p_l(\mathbf{x}_k) = g(\mathbf{x}_k), k = n_i+1, 2, \ldots, n, \tag{10}$$

$$\sum_{j=n_i+1}^{n} \alpha_j \mathbf{B}p_l(\mathbf{x}_j) = 0, l = 1, 2, \ldots, w. \tag{11}$$

Rearranging (8)–(11), we have the following block matrix system

$$\begin{bmatrix} \phi_{n_i n} & \mathbf{Q}_{n_i w} \\ \mathbf{B}\Phi_{n_b n} & \mathbf{BP}_{n_b w} \\ [\mathbf{Q}^T_{n_i w}, (\mathbf{BP})^T_{n_b w}] & \mathbf{0}_{ww} \end{bmatrix} \begin{bmatrix} \alpha_1 \\ \vdots \\ \alpha_{n+w} \end{bmatrix} = \begin{bmatrix} \mathbf{f}_{n_i} \\ \mathbf{g}_{n_b} \\ \mathbf{0}_w \end{bmatrix}, \tag{12}$$

where the sub-indexes of the matrices and the vectors indicate the sizes of the matrices and the vectors. The undetermined coefficients $\{\alpha_j\}_{j=1}^{n+w}$ can be obtained by solving the above linear system.

A key feature of MAPS is that the particular solutions of a differential equation with a chosen RBF need to be derived analytically. In the literature, particular solutions for various differential operators for some commonly used RBFs have been derived [9, 11]. A list of the particular solutions with respect to PS and MQ for the Laplacian Δ in $\mathbf{R}^2$ and $\mathbf{R}^3$ are listed in Tables II and III.

One may notice that the particular solution of $\Delta\Phi(r) = \phi(r)$ is a commonly used RBF in MAPS where $\phi(r)$ is an mth order PS. Even though the Laplacian operator is a self-adjoint operator, we cannot claim that the basis we are using is just the (m+1)th order of PS. The reason is the following:

Consider the simplest elliptic PDE of form

$$\Delta u = f$$

in which

$$\langle f, \phi \rangle = \langle \Delta u, \phi \rangle = \langle u, \Delta \phi \rangle.$$

This implies the solution to the PDE is approximated in functional space $\Delta\phi$ which is equivalent to PS of order $m-2$. This is not the case in our article, as we are approximating the solution u by a PS of order $m+2$ with additional r^{2m+2}, in addition to the orthogonal polynomial basis.

However, in some instances, when solutions to (5) are not available with respect to a given RBF, the MAPS procedure discussed above cannot be directly utilized. To alleviate this difficulty, a new formulation of (1) is needed:

$$\mathbf{L}'u(\mathbf{x}) = f(\mathbf{x}) + \left(\mathbf{L}' - \mathbf{L}\right) u(\mathbf{x}), \tag{13}$$

where the differential operator $\mathbf{L}'$ is chosen so that a particular solution $\Phi(r)$ for $\mathbf{L}'$ with respect to the given RBF $\phi(r)$ is known, that is,

$$\mathbf{L}'\Phi(r) = \phi(r). \tag{14}$$

Then MAPS can be applied to (13). In our initial development of the method, the basis is chosen from $L\Phi(r) = \phi(r)$, where Φ is a particular solution obtained analytically, which can be done when differential operator L and chosen RBF ϕ are simple enough. However, this is not very practical for most of PDEs we are dealing with in the real application. So we extend the idea above to the main operator L' in the operator L, for example when $L = \Delta + \partial/\partial x$, we chose $L' = \Delta$. As previously demonstrated, for any $\mathbf{x}_k \in \Omega$, we interpolate the right-hand side of (13),

$$\sum_{j=1}^{n} \alpha_j \phi(\|\mathbf{x}_k - \mathbf{x}_j\|) + \sum_{l=1}^{w} \alpha_{n+l} q_l(\mathbf{x}_j) = \mathbf{L}'\hat{u}(\mathbf{x}_k). \tag{15}$$

Therefore, from (14), we have

$$\sum_{j=1}^{n} \alpha_j \Phi(\|\mathbf{x}_k - \mathbf{x}_j\|) + \sum_{l=1}^{w} \alpha_{n+l} p_l(\mathbf{x}_j) = \hat{u}(\mathbf{x}_k), \tag{16}$$

where

$$\mathbf{L}' p_l(\mathbf{x}) = q_l(\mathbf{x}), \qquad l = 1, 2, \cdots, w. \tag{17}$$

Then (13) becomes a linear system in Ω:

$$\mathbf{L}\hat{u}(\mathbf{x}_k) = \sum_{j=1}^{n} \alpha_j \mathbf{L}\Phi(\|\mathbf{x}_k - \mathbf{x}_j\|) + \sum_{l=1}^{w} \alpha_{n+l} \mathbf{L} p_l(\mathbf{x}_j) = f(\mathbf{x}_k), k = 1, 2, \ldots, n_i, \tag{18}$$

$$\sum_{j=1}^{n_b} \alpha_j \mathbf{L} p_l(\mathbf{x}_j) = 0, l = 1, 2, \ldots, w, \tag{19}$$

and on the boundary $\partial\Omega$

$$\mathbf{B}\hat{u}(\mathbf{x}_k) = \sum_{j=1}^{n} \alpha_j \mathbf{B}\Phi(\|\mathbf{x}_k - \mathbf{x}_j\|) + \sum_{l=1}^{w} \alpha_{n+l} \mathbf{B} p_l(\mathbf{x}_j) = g(\mathbf{x}_k), k = n_i + 1, 2, \ldots, n, \tag{20}$$

$$\sum_{j=1}^{n_b} \alpha_{n_i+j} \mathbf{B} p_l(\mathbf{x}_j) = 0, l = 1, 2, \ldots, w. \tag{21}$$

Rearranging (18)–(21), we can rewrite them in the following block matrix form

$$\begin{bmatrix} \mathbf{L}\Phi & \mathbf{LP} \\ \mathbf{B}\Phi & \mathbf{BP} \\ [\mathbf{LP}^T, (\mathbf{BP})^T] & \mathbf{0} \end{bmatrix} \begin{bmatrix} \alpha_1 \\ \vdots \\ \alpha_{n+q} \end{bmatrix} = \begin{bmatrix} \mathbf{f} \\ \mathbf{g} \\ \mathbf{0} \end{bmatrix}. \tag{22}$$

Compared to the original MAPS using MQ, there are additional q degrees of freedom, which is usually much smaller than the number of data points n in the domain. Thus, little additional computational resource is required for the proposed modified MAPS. In the next section, we will numerically demonstrate the high accuracy of the modified MAPS on complicated PDE linear and nonlinear problems with variable coefficients on irregular domains.

III. NUMERICAL RESULTS

To illustrate the effectiveness of our proposed approach, we consider several two-dimensional and three-dimensional problems on irregular domains. Throughout this section, n_i denotes the number of nodes in the domain Ω, n_b the number of nodes on the boundary $\partial\Omega$, $n = n_i + n_b$ the total number of points, and n_t the number of randomly selected test points on the boundary and inside the domain. We try to distribute the boundary and interior points as uniformly as we can in the computational process. The root mean squared error, the maximum absolute error, and the maximum relative absolute error are defined as follows:

$$\varepsilon_\infty = \max_{k=1}^{n_t} |\hat{u}_k - u_k|, \qquad \varepsilon_2 = \sqrt{\frac{1}{n_t} \sum_{k=1}^{n_t} (\hat{u}_k - u_k)}, \qquad \varepsilon_{rel} = \max_{k=1}^{n_t} |\frac{\hat{u}_k - u_k}{u_k}|,$$

where $\hat{u}_k = \hat{u}(\mathbf{x}_k)$ is the approximated solution, and $u_k = u(\mathbf{x}_k)$ is the exact solution. We examine the proposed modified MAPS using PS and MQ on two second-order variable coefficients linear PDEs on complicated irregular domains in 2D and 3D. To distinguish the techniques in the modified MAPS from the original MAPS, we list the key components in the algorithms:

1. RBF Basis: RBF (Kansa's Method) or integrated RBF (MAPS);
2. Polynomial basis: included on top of the RBF (modified MAPS) or not included for RBFs other than polyharmonic splines (original MAPS);
3. Basis with the shape parameters (MQ) or without the shape parameters (PS).

Throughout the following five examples, we compared the different combinations of those key components in terms of accuracy and rate of convergence for various kinds of elliptic PDEs.

Example 1. To demonstrate that proposed method with PS is effective in term of accuracy compared to original Kansa's method using MQ, we perform the stress tests for the following Poisson equation with large forcing term:

$$\Delta u(x, y) = 41 e^{-4x+5y}, \qquad (x, y) \in \Omega, \tag{23}$$

$$u(x, y) = e^{-4x+5y}, \qquad (x, y) \in \partial\Omega, \tag{24}$$

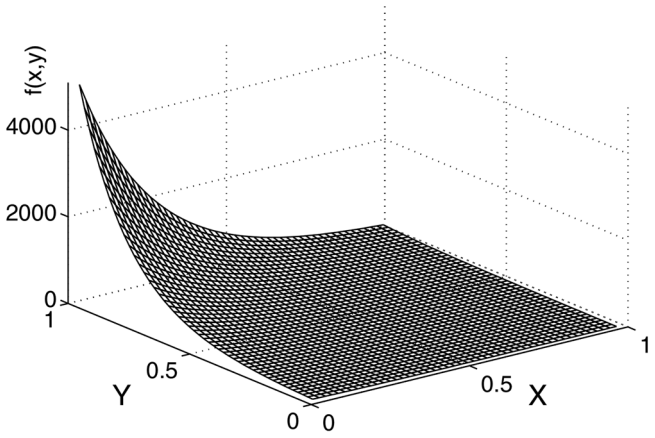

FIG. 1. Example 1: The profile of the forcing term $f(x, y)$.

where Ω is the unit square domain. The exact solution is given by

$$u_{\text{exact}}(x, y) = e^{-4x+5y}, \qquad (x, y) \in \Omega \cup \partial\Omega.$$

The profile of the forcing term $f(x, y)$ is shown in Figure 1. We note that the range of forcing term is between 0 and 4416. It is a challenge to obtain even a reasonable result under such large forcing term.

In the numerical implementation, we choose 324 uniformly distribute interior points and 76 boundary points. To measure the accuracy, we choose 784 uniformly distributed test points inside the domain. In Table IV, we observe excellent results using various orders of polyharmonic splines. We note that the accuracy keep improving for higher order of polyharmonic splines. Conversely, we compare with the Kansa's method [14] using normalized MQ ($\sqrt{1 + r^2c^2}$) as the basis. In this test, we use exactly the same number of boundary, interior, and test points as mentioned above. In such case, we can only achieve accuracy of 1.59×10^{-3} for the best choice of the shape parameter $c = 1.986$. There is a sharp contrast in accuracy using the polyharmonic splines and normalized MQ which considered to be one of the best RBFs.

Example 2. In this example, we consider the Poisson equation with Dirichlet boundary condition in the square domain $[-1, 1]^2$. The forcing term and boundary condition are given based on the analytical solution $u(x, y) = 1/(1 + 25(x^2 + y^2))$, see Figure 2. It is well known that such function appears to form the Runge's phenomena wherein the approximation errors near the end of the data support at ± 1 can become unacceptably large. We will compare the performance of proposed method using PS with MQ, when the polynomial basis functions are added in both cases. The evenly spaced interior and boundary nodes are used: $n_i = 784$, $n_b = 116$, and the number of randomly distributed test points is $n_t = 1024$.

Table V shows the corresponding maximum absolute errors and the root mean squared errors using MAPS with various orders of PS and MQ with the same order of polynomial basis. We observe that PS clearly outperforms MQ in terms of accuracy when the order of polynomials is between 2 and 4. The shape parameter in MQ plays an important role in terms of accuracy of MAPS. We tested multiple values of c between 0.001 and 10, and found that MAPS performs

TABLE IV. Example 1: $\varepsilon_\infty and \varepsilon_2$ using various orders m of PS.

m	ε_∞	ε_2
5	4.01×10^{-4}	1.34×10^{-4}
7	1.07×10^{-4}	3.48×10^{-5}
9	2.83×10^{-6}	9.22×10^{-7}
11	5.40×10^{-7}	1.09×10^{-8}
13	5.09×10^{-8}	6.14×10^{-9}
15	2.40×10^{-8}	4.70×10^{-9}

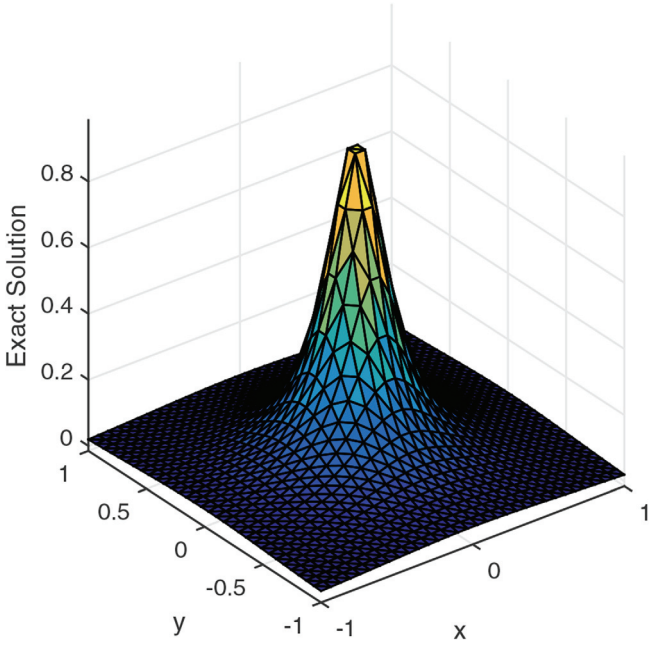

FIG. 2. Example 2: The profile of the analytical solution. [Color figure can be viewed at wileyonlinelibrary.com]

TABLE V. Example 2: ε_∞ and ε_2 using various orders of PS and MQ in MAPS, with $n_i = 784, n_b = 116, n_t = 1024$.

	PS		MQ		
m	ε_∞	ε_2	ε_∞	ε_2	c
1	2.49×10^{-3}	1.65×10^{-4}	1.40×10^{-2}	9.90×10^{-4}	0.001
2	3.55×10^{-4}	3.11×10^{-5}	1.40×10^{-2}	9.90×10^{-4}	0.001
3	1.80×10^{-4}	2.25×10^{-5}	1.40×10^{-2}	9.90×10^{-4}	0.001
4	1.58×10^{-4}	2.60×10^{-5}	1.40×10^{-2}	9.90×10^{-4}	0.001
5	1.83×10^{-3}	4.20×10^{-4}	1.40×10^{-2}	9.90×10^{-4}	0.001

better using MQ when c is small. As shown in Table V the best results using PS is in the order of magnitude 10^{-5}. The results using MQ tend to stay at the same level of accuracy. We suspect the effect of the polynomial basis in MAPS when we use MQ is not much. However, when the polynomial degree is higher, the method is more stable using MQ than using PS.

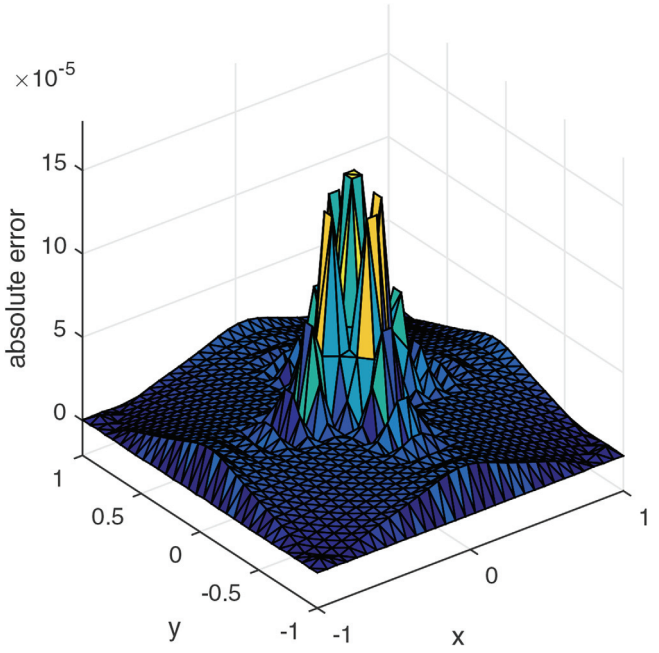

FIG. 3. Example 2: The profile of the approximate solution and the absolute error using MAPS with PS of order 4. [Color figure can be viewed at wileyonlinelibrary.com]

Figure 3 shows the absolute errors of the approximate solutions using PS of order 4. Note that a low order of polynomial basis is used. In this situation, a higher order polynomial basis will not perform better. In fact, order 2, 3, and 4 of polynomials performs similar, but others do not work well.

Note that we used about 31 equal spaced interpolation points in each axis direction, the order of polynomial basis $m = 4$ indicates we are trying to approximation the solution by a solutions space formed by PS and polynomial basis of degree 4. However, we still achieve reasonable accuracy (order of 10^{-5}) in the approximation of the solutions to the PDE. In general, the oscillation at the edges of an interval occurs even when 5th polynomial is used over a set of equispaced interpolation points.

Example 3. In this example, we consider the following PDE with variable coefficients

$$\Delta u + x^2 y u + y^3 \sin(x)\frac{\partial u}{\partial x} - y^2 \cos(x)\frac{\partial u}{\partial y} = f(x, y), \quad (x, y) \in \Omega, \tag{25}$$

$$u(x, y) = y\cos(x) + x\cos(y), \quad (x, y) \in \partial\Omega, \tag{26}$$

where $f(x, y)$ is given according to the following analytical solution

$$u(x, y) = y\cos(x) + x\cos(y), \qquad (x, y) \in \Omega \cup \partial\Omega. \tag{27}$$

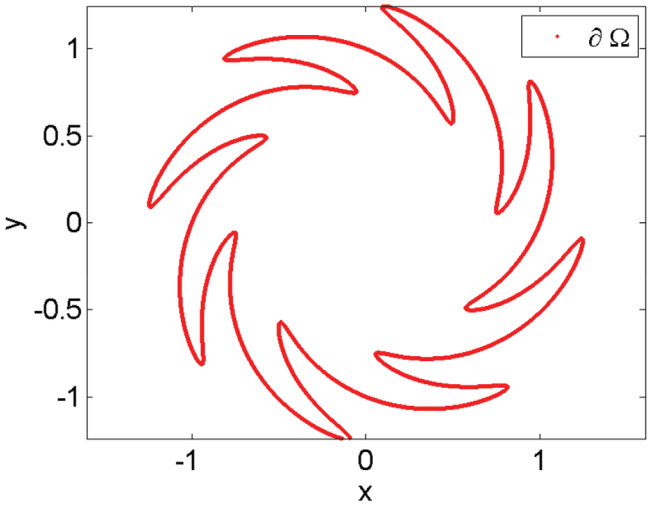

FIG. 4. Example 3: The profile of the gear-shape domain and the absolute error using MAPS with PS of order 10. [Color figure can be viewed at wileyonlinelibrary.com]

The gear-shape domain is defined by the following parametric equation:

$$\partial\Omega = \left\{(x,y) : x = \rho(\theta)\cos\left(\theta + \frac{1}{2}\sin(8\theta)\right),\ y = \rho(\theta)\sin\left(\theta + \frac{1}{2}\sin(8\theta)\right), 0 \le \theta \le 2\pi\right\}, \tag{28}$$

where

$$\rho(\theta) = \frac{1}{2}\left(2 + \frac{1}{2}\sin(8\theta)\right). \tag{29}$$

The profile of the gear-shape domain is shown in Figure 4. The domain has eight sharp corners which are generally difficult to simulate with mesh-based methods. It is indeed a challenge to solve such a PDE with variable coefficients, especially on complicated domains with sharp corners.

For the numerical implementation, we choose uniformly distributed interior points $n_i = 834$, boundary points $n_b = 250$, and randomly distributed test points $n_t = 340$. Table VI shows the corresponding maximum absolute errors and the root mean squared errors using MAPS with various orders of PS and MQ. We observe that PS clearly outperforms MQ in terms of accuracy. When utilizing other RBFs containing shape parameters, we need to justify the shape parameter to find an 'optimal' choice which leads to an "optimal" approximate solution. This is still an outstanding research topic. To make sure to have a fair comparison, we have done our best to find a good shape parameter. In fact, for some reason the shape parameter of MQ is insensitive in this case. Conversely, when we use PS in the modified MAPS, we can simply increase the order of PS to improve the accuracy. With a small amount of collocation points and a high order PS, a numerical accuracy of 10^{-10} can be easily achieved. The additional computational cost is marginal comparing to a lower order PS and the original MAPS.

Table VII shows the maximum absolute errors and the root mean squared errors with various numbers of collocation points and MQ and PS of order $m = 3$, where the number of test points

TABLE VI. Example 3: $\varepsilon_\infty and \varepsilon_2$ using various orders of PS and MQ in MAPS, with $n_i = 834, n_b = 250, n_t = 340$.

	PS		MQ		
m	ε_∞	ε_2	ε_∞	ε_2	c
1	3.92×10^{-3}	1.29×10^{-3}	2.02×10^{-1}	4.87×10^{-2}	2
3	4.88×10^{-5}	1.18×10^{-5}	1.34×10^{-2}	3.87×10^{-3}	2
5	1.13×10^{-5}	2.31×10^{-6}	2.20×10^{-3}	5.91×10^{-4}	2
7	2.63×10^{-7}	3.78×10^{-8}	3.71×10^{-6}	8.57×10^{-7}	2
10	7.30×10^{-10}	6.92×10^{-11}	6.33×10^{-8}	1.49×10^{-8}	1.5

TABLE VII. Example 3: ε_∞ and ε_2 using different numbers of boundary and interior points, n_b and n_i, with PS and MQ in MAPS, where $n_t = 340, m = 3$.

		PS		MQ		
n_b	n_i	ε_∞	ε_2	ε_∞	ε_2	c
250	834	4.88×10^{-5}	1.18×10^{-5}	1.34×10^{-2}	3.87×10^{-3}	2
250	3342	4.35×10^{-5}	1.37×10^{-5}	2.66×10^{-2}	5.64×10^{-3}	2
250	7498	9.91×10^{-5}	1.54×10^{-5}	5.07×10^{-2}	1.29×10^{-2}	2

is $n_t = 340$. Further increasing the number of collocation points will increase the computational cost, but there is little or no improvement in terms of accuracy. Furthermore, if we increase the order of PS to 4 ($m = 4$), the numerical accuracy will improve compared to PS of order 3. Thus, to achieve higher accuracy, we recommend increasing the order of PS. With $m = 3$, the results from MQ cannot compete with PS no matter what value the shape parameter c is used. To obtain a reasonable numerical result using MQ, we recommend to use a higher degree of augmented polynomial basis.

The Cauchy problem for an elliptic equation is a classical ill-posed problem and occurs in many important applications. Even if some of the theoretical investigations are quite general, the numerical procedures proposed are typically for the two-dimensional case and often only valid for the problem with constant coefficients. To the best of our knowledge, it is rare in the literature to treat the numerical solutions of elliptic Cauchy problems in three dimensions with all three coefficients depending on (x, y, z), and achieve high accuracy in irregular domains. We consider such problems in the following example.

Example 4. In this example, we propose to examine MAPS with PS and MQ on an ill-posed Cauchy problem for an elliptic PDE with variable coefficients in 3D as follows:

$$(au_x)_x + (bu_y)_y + (cu_z)_z = f(x, y, z), \qquad (x, y, z) \in \Omega, \tag{30}$$

$$u(x, y, z) = e^{x+y+z}, \qquad (x, y, z) \in \partial\Omega_1, \tag{31}$$

$$u_x(x, y, z) = e^{x+y+z}, \qquad (x, y, z) \in \partial\Omega_2, \tag{32}$$

where $a(x, y, z) = xyz + 1$, $b(x, y, z) = x(y + 1) + 1$, $c(x, y, z) = x + y + z + 1$, and $f(x, y, z)$ is given according to the following analytical solution

$$u(x, y, z) = e^{x+y+z}, \quad (x, y, z) \in \Omega \cup \partial\Omega_1 \cup \partial\Omega_2. \tag{33}$$

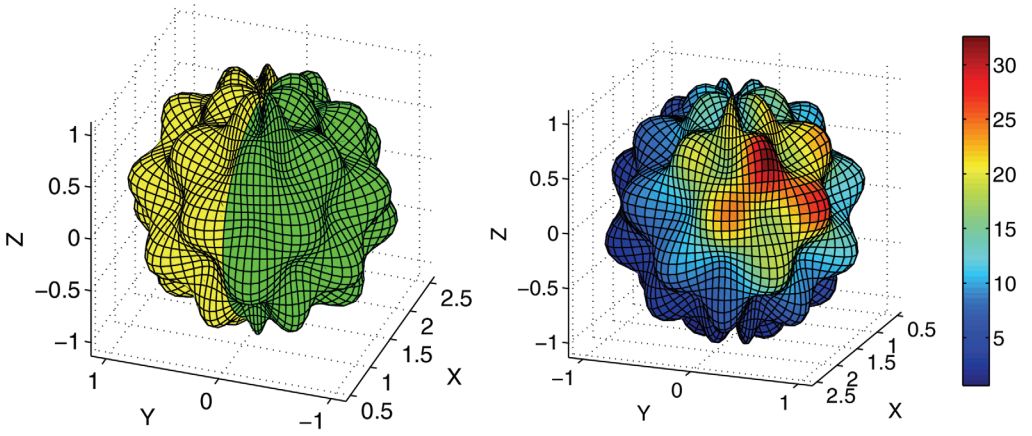

FIG. 5. Example 4: (Left) The profile of the bumpy sphere containing $\partial\Omega_1$ (yellow surface) and $\partial\Omega_2$ (green surface). (Right) The profile of the exact solution on the boundary surface. [Color figure can be viewed at wileyonlinelibrary.com]

The parametric equation of the surface of the domain, which is known as the bumpy sphere, is defined as follows:

$$\begin{aligned}\partial\Omega_1 \cup \partial\Omega_2 = \{(x,y,z) :\ & x = \rho\sin(\phi)\cos(\theta) + 1.5, \quad 0 \le \theta \le 2\pi,\\ & y = \rho\sin(\phi)\sin(\theta), \quad 0 \le \phi \le \pi,\\ & z = \rho\cos(\phi), \quad \rho = 1 + \sin(5\theta)\sin(7\phi)/5\}.\end{aligned}$$

Note that $\partial\Omega_1$ is the surface where $y \ge 0$, and $\partial\Omega_2$ the surface where $y < 0$. Figure 5 (left) shows the profile of the boundary surface of the bumpy sphere where $\partial\Omega_1$ is colored with a yellow surface and $\partial\Omega_2$ a green surface. On the right side of Figure 5, we show the profile of the exact solution on the boundary surface.

Table VIII shows the maximum absolute errors and the root mean squared errors using MAPS with various orders of PS and MQ, where $n_i = 3948$, $n_b = 1000$, and $n_t = 9488$. Table IX shows similar results using $n_i = 1295$, $n_b = 500$, and $n_t = 441$. By comparing those two tables, we see that numerical accuracy is similar when a higher order of polynomial basis is used, even though the number of collocation points in Table IX is much smaller. Similar to our previous example, the numerical accuracy improved dramatically with a higher order of PS. With a small amount of collocation points and a higher order of PS ($m = 15$), the numerical accuracy can be easily reached to an order of 10^{-8} in 3D which is significant. The accuracy obtained using MQ is slightly better than the one shown in Example 1. However, the accuracy is still low if a lower order polynomial basis is used. In addition, we have made an effort to find an appropriate shape parameter c for MQ which is very time-consuming. The PS has a clear advantage than the MQ in this case.

Table X shows the errors using the modified MAPS with various numbers of collocation points. Further increasing the number of collocation points will improve the numerical accuracy in 3D, but the rate is not as rapid as increasing the order of PS. The modified MAPS with MQ produces acceptable numerical results (order of 10^{-2}) as we can see from many literature for a 3D problem on an irregular domain. But the modified MAPS with PS produces an order of 10^{-3} error using only a small number of interior and boundary collocation points. Furthermore, we can easily

TABLE VIII. Example 4: $\varepsilon_\infty and \varepsilon_2$ using various orders, m of PS and MQ in MAPS, with $n_i = 3948, n_b = 1000, n_t = 9488$.

	PS		MQ		
m	ε_∞	ε_2	ε_∞	ε_2	c
7	9.83×10^{-5}	7.45×10^{-6}	4.65×10^{-1}	6.38×10^{-2}	0.001
10	1.45×10^{-5}	7.45×10^{-7}	4.73×10^{-2}	5.70×10^{-3}	0.001
12	3.36×10^{-7}	1.79×10^{-8}	2.93×10^{-4}	1.97×10^{-5}	0.001
15	2.08×10^{-7}	1.01×10^{-8}	7.74×10^{-7}	4.45×10^{-8}	0.001

TABLE IX. Example 4: ε_∞, ε_2 and ε_{rel} using different orders, m of PS and MQ in MAPS, with $n_i = 1295, n_b = 500, n_t = 441$.

	PS		MQ		
m	ε_∞	ε_2	ε_∞	ε_2	c
7	1.66×10^{-3}	1.57×10^{-4}	3.24×10^{-1}	4.33×10^{-2}	0.1
10	9.28×10^{-5}	6.27×10^{-6}	5.01×10^{-3}	5.91×10^{-4}	0.1
12	3.42×10^{-6}	2.99×10^{-7}	6.50×10^{-4}	6.31×10^{-5}	0.1
15	5.91×10^{-7}	3.77×10^{-8}	1.70×10^{-6}	1.79×10^{-7}	0.1

TABLE X. Example 4: $\varepsilon_\infty and \varepsilon_2$ using various numbers of boundary and interior points with PS and MQ in MAPS, where $n_t = 9488, m = 7$.

		PS		MQ		
n_b	n_i	ε_∞	ε_2	ε_∞	ε_2	c
250	163	5.57×10^{-3}	6.83×10^{-4}	1.05×10^{-1}	1.22×10^{-2}	0.1
500	1120	6.26×10^{-4}	4.07×10^{-5}	2.90×10^{-1}	4.72×10^{-2}	0.1
500	1295	1.66×10^{-3}	1.57×10^{-4}	3.24×10^{-1}	4.33×10^{-2}	0.1
750	2205	7.29×10^{-4}	4.88×10^{-5}	7.58×10^{-1}	1.17×10^{-1}	0.1
1000	3948	9.83×10^{-5}	7.45×10^{-6}	4.65×10^{-1}	6.38×10^{-2}	0.001

improve the accuracy using more collocation points or higher order PS. Figure 6 shows the rate of convergence of the modified MAPS using PS of order 7 and we observe a quadratic rate of convergence.

To further demonstrate the effectiveness of the proposed improved MAPS, we consider the well-known Stanford Bunny as the computational domain whose boundary data points are available at the website of the Stanford Computer Graphics Laboratory [22]. We consider the same differential equation as above. In the following test, 1899 boundary collocation points, 690 interior points, and 2345 interior test points are used. The profile of the Stanford Bunny and 1889 scanned boundary points are shown in Figure 7 (left) and the exact solution on the surface of the domain (right). We consider the front side of the Bunny as $\partial\Omega_1$ which contains the first half of boundary data points. The other half of boundary points reside on $\partial\Omega_2$ which is the back side of the Bunny. Furthermore, since the scale of the original data from the Bunny is too small, we enlarge all the above data by 10 times. In Table XI, we show the results of using PS and MQ with orders 8, 10, and 12. Despite the extremely complicated geometric shape of the domain, the accuracy remains excellent.

Example 5. In this example, we consider the following nonlinear Poisson-type problem:

$$\Delta u(x, y) = 3u^2, \qquad (x, y) \in \Omega, \tag{34}$$

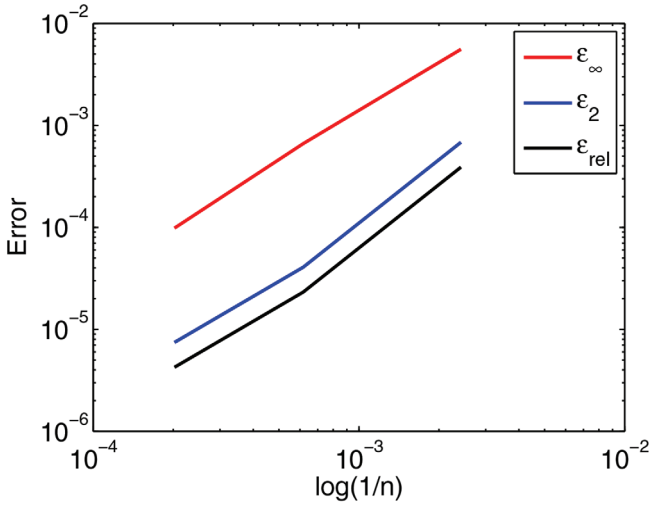

FIG. 6. Example 4: The rate of convergence of MAPS with PS of order 7. [Color figure can be viewed at wileyonlinelibrary.com]

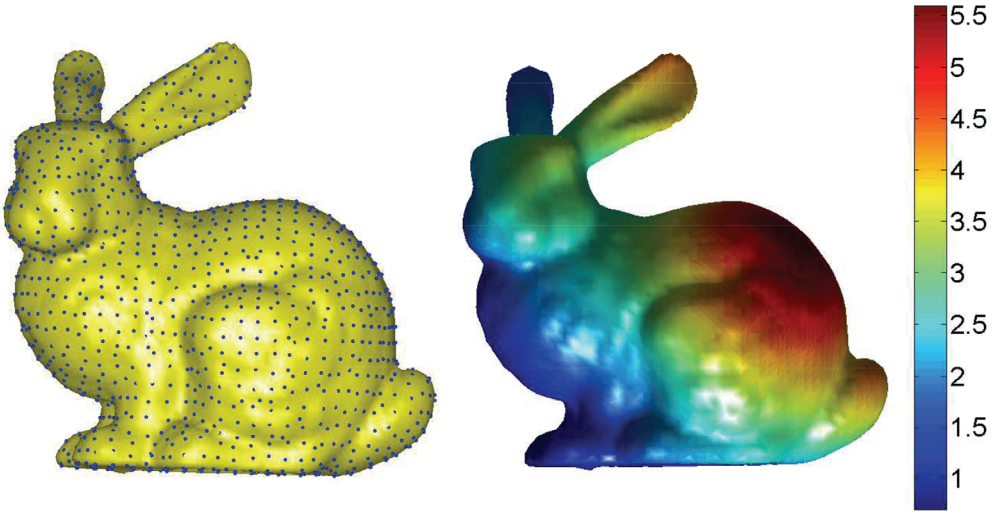

FIG. 7. Example 4: The profile of the Stanford Bunny and its 1889 boundary points (left) and the exact solution on the surface of the domain (right). [Color figure can be viewed at wileyonlinelibrary.com]

$$u(x, y) = g(x, y), \qquad (x, y) \in \partial\Omega, \tag{35}$$

where Ω is the unit square domain and $g(x, y)$ is given based on the exact solution

$$u_{\text{exact}}(x, y) = \frac{4}{(3 + x + y)^2}, \quad (x, y, z) \in \Omega \cup \partial\Omega.$$

For the implementation, we choose 324 interior points and 116 boundary points both uniformly distributed inside the square domain and its boundary. We use direct Picard method for

TABLE XI. Example 4: ε_∞ and ε_2 using various orders m of PS and MQ in MAPS with $n_i = 690, n_b = 1889, n_t = 2345$ in the Stanford Bunny domain.

	PS		MQ		
m	ε_∞	ε_2	ε_∞	ε_2	c
8	1.30×10^{-9}	6.91×10^{-11}	1.37×10^{-5}	1.72×10^{-5}	0.001
10	7.78×10^{-11}	4.20×10^{-12}	1.02×10^{-5}	1.29×10^{-6}	0.001
12	1.93×10^{-9}	4.66×10^{-11}	1.41×10^{-7}	1.35×10^{-8}	0.001

TABLE XII. Example 5: $\varepsilon_\infty and \varepsilon_2$ using various orders m of PS.

m	ε_∞	ε_2
5	2.96×10^{-9}	1.62×10^{-9}
7	2.73×10^{-9}	1.43×10^{-9}
9	2.75×10^{-9}	1.44×10^{-9}
11	2.69×10^{-9}	1.41×10^{-9}
13	2.16×10^{-8}	5.51×10^{-9}

the nonlinear iteration. We set the initial guess value $u_0(x, y) = 0$ for all $(x, y) \in \Omega$. When $\|u_{i+1} - u_i\| < 10^{-7}$, we stop the iteration and take u_{i+1} as the approximate solution of (34)–(35). In Table XII, we show the numerical results using various orders of polyharmonic splines. From the table, we again observe very high accuracy of the modified MAPS with PS of order up to 13. When the order becomes higher, the accuracy will not improve anymore.

Example 6. In this example, we consider the following blow-up problem [23]

$$\Delta u = -\delta e^u, \text{ in } \Omega, \tag{36}$$

$$u = 0, \text{ on } \partial\Omega. \tag{37}$$

It is shown that the existence of the solution of the above problem depends on the value of δ. There is a critical value, δ^* such that if $\delta < \delta^*$ there is a positive solution, whereas if $\delta > \delta^*$ there exists no solution. In [24], the authors showed that if $\delta > \delta^*$ the solution of the time dependent problem becomes infinite in finite time irrespective of initial values. As the critical values generally cannot be computed analytically, especially when the domain of the PDE is complicated, we usually resort to numerical methods to approximate δ^*. In the past, both the finite element method (FEM) and boundary element method (BEM) have been used for this purpose. In [23], the author used the method of fundamental solutions (MFS) to approximate δ^* in comparison with BEM and FEM. In this article, we will use the MAPS with PS to estimate δ^*. The monotone iteration introduced in [23] is used.

Table XIII shows the critical values the problem when three different geometric shapes of domain Ω, a square of $[0, 2] \times [0, 2]$ the unit circle, and an ellipse with semi-major axis 2 and semi-minor axis 1, are used. The MAPS with PS is used to solve the nonhomogeneous Poisson equation at each iteration. Our method estimates the critical value with a higher accuracy than what was reported in [23].

Next, we will test the convergence rate numerically at a particular point. A profile of the solution when $\delta = 1.703863$ is shown in Figure 8. The maximum value of the solution appears at the center of the domain. We will focus on the center of the regular square domain $[0, 2]^2$ to eliminate the effect the domain shape to the convergence rate. Specifically, we will estimate $u(1, 1)$ with different minimum distance between nodes. When the nodes become denser, a smaller degree of

TABLE XIII. Example 6: critical values δ^* using PS of order $5tolerance10^{-10}$ on different shapes of Ω.

Shape	n_i	n_b	BEM	FEM	MFS	MAPS	Exact
Square	361	236	1.770	1.703	1.703	1.701	1.7
Circle	305	120	2.031	2.001	2.001	2.000	2
Ellipse	242	120	1.252	1.234	1.235	1.2315	–

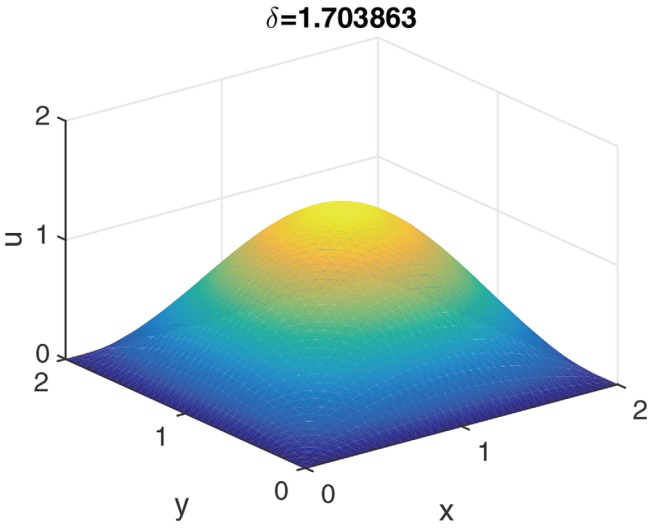

FIG. 8. Example 6: The profile of the solution on the square domain when $\delta = 1.703863$. [Color figure can be viewed at wileyonlinelibrary.com]

polynomial basis will be required. We will use a polynomial of degree 2, 4, and 6 to conduct the convergence analysis so that denser nodes can be tested. Table XIV shows the rate of convergence, where $|u_i - u_{i-1}|$ is obtained by absolute difference between estimated $u(1, 1)$ on two consecutive h is used, and ratio is the ratio between two consecutive absolute errors. A rate of convergence of quadruple convergence is expected when 4-th order polynomial basis is used. When the order of polynomial basis increases, the rate of convergence decreased. Thus, when accuracy is a critical aspect, we suggest to use higher order polynomial basis, but lower order polynomial is preferred if we want fast convergence.

As our method is a global method, which uses all given discrete points in the domain to create a large dense matrix. Thus, the efficiency of the method when given many points is poor, especially in MATLAB. We will need a more sophisticated computer language or to improve the method to a local method for improvement in computational efficiency. This will be our ongoing research topic.

IV. CONCLUSION

In the past, PS RBF has not been used in MAPS due to the low performance in terms of accuracy. In this article, we modified MAPS so conditionally positive definite PS RBF can be utilized to solve various kinds of elliptic PDEs in two- and three-dimensional space. In the modified MAPS, an additional polynomial basis is used in addition to the integrated RBFs. Thus, other RBFs such

TABLE XIV. Example 6: rate of convergence at $u(1,1)\, for \delta = 1$ using PS of order 2, 4, and 6 on a square domain $[0,2]^2$, where $|u_i - u_{i-1}|$ is obtained by absolute difference between estimated $u(1,1)$ on two consecutive h is used, and ratio is the ratio between two consecutive absolute errors.

m	h	$u(1,1)$	$\lvert u_i - u_{i-1}\rvert$	Ratio
2	1/4	0.3749		
	1/8	0.3919	0.0170	
	1/16	0.3947	0.0028	6.0714
	1/32	0.3953	0.0006	4.6667
4	1/2	0.3544		
	1/4	0.3807	0.0263	
	1/8	0.3924	0.0117	2.2479
	1/16	0.3948	0.0024	4.8750
	1/32	0.3954	0.0006	4.0000
6	1/4	0.3830		
	1/8	0.3924	0.0094	
	1/16	0.3949	0.0025	3.7600

as MQ can be used in the modified MAPS as well. The difference between the original and the modified MAPS is that a low-order polynomial basis needs to be added into the kernels in the modified method. The polynomial basis is needed for PS to overcome the invertibility issues of the collocation matrix. However, the original MAPS does not require additional polynomial basis to the particular solution basis (integrated RBFs). Furthermore, we add a polynomial basis to the kernels instead of integrating it like the original MAPS. To our surprise, PS outperforms MQ in almost all of the numerical examples we tested.

There are many ways to select the basis functions for the RBF collocation methods. In the past, among all kinds of RBFs, MQ is considered to be the best and the most effective and commonly used RBFs. However, the quest of the optimal shape parameter for all types of RBFs including MQ is still an outstanding research problem. Conversely, there is no shape parameter in PS. Thus, the difficult issue of searching for the optimal shape parameter in MQ is alleviated. For scatter data interpolation, we found the high order polyharmonic splines with high degree of augmented polynomials have the negative effect on the accuracy. However, for solving PDEs, we obtain very high accuracy for high order of integrated polyharmonic splines with additional polynomial basis. The results using particular solution derived from polyharmonic splines with augmented polynomial basis functions are normally superior to MQ. The original MAPS with PS requires integration of additional augmented polynomial basics. The modified MAPS simply uses integrated RBFs with non-integrated polynomial basis, which resulted in better accuracy from PS than from MQ. With such high accuracy for solving PDEs, polyharmonic splines is expected to gain more popularity in the future.

To improve the accuracy of the modified MAPS using PS, we found through our numerical experiments, that we can (i) use more collocation points or (ii) use a higher order PS as the basis. The numerical study indicates that the proposed method has high computational accuracy with little additional computational cost comparing to other RBFs. The higher degree polynomial is notorious in numerical implementation. We overcome the difficulty of implementing polynomials with high degrees in our method. To our knowledge, this is the first time polyharmonic splines with polynomial basis up to degree 15 has been implemented to solve the given PDEs.

We have noticed that the polynomial basis plays an important role in our approximation to solutions to the PDEs. However, with polynomial basis only without polyharmonic splines, the

numerical interpolation to an even analytical function failed numerically due to the highly ill-conditioning of the resultant matrix. However, combine with the polyharmonic splines and even with high order of polynomial terms, it works out nicely.

We believe that the selection of particular solutions derived from polyharmonic splines together with polynomial basis provide tremendously advantages in terms of accuracy without loss of efficiency. However, the global dense linear system generated by MAPS is costly in computation. We will future focus on localization of the method to improve the efficiency. Conversely, there are full of theoretical justification in the context of data interpolation using polyharmonic spline [19, 20, 25–27]. The theoretical justification of polyharmonic splines for solving PDEs is another open question that is worthy for further investigation.

ACKNOWLEDGMENT

The authors wish to thank Prof. Scott Fulton and Prof. Guohui Song for useful discussions. We also greatly appreciate the referees for their constructive comments and suggestions which results in an improved manuscript.

References

1. M. D. Buhmann, Multivariate cardinal interpolation with radial basis functions, Constr Approx 6 (1990), 225–255.
2. M. D. Buhmann, Radial basis functions, theory and implementations, Cambridge University Press, Cambridge, U. K., 2003.
3. C. S. Chen, Y. C. Hon, and R. A. Schaback, Scientific computing with radial basis functions, Technical Report, Department of Mathematics, University of Southern Mississippi, Hattiesburg, MS 39406, USA, preprint, 2005.
4. G. E. Fasshauer, Solving partial differential equations by collocation with radial basis functions, A. L. Mehaute, C. Rabut, and L. L. Schumaker, editors, Surface fitting and multiresolution methods, Vanderbilt University Press, Nashville, TN, 1997, pp. 131–138.
5. A. I. Tolstykh and D. A. Shirobokov, On using radial basis functions in a "finite difference" mode with applications to elasticity problems, Comput Mech 33 (2003), 68–79.
6. C. S. Chen, C. M. Fan, and P. H. Wen, The method of particular solutions for solving elliptic problems with variable coefficients, Int J Comput Methods 8 (2011), 545–559.
7. C. S. Chen, C. M. Fan, and P. H. Wen, The method of particular solutions for solving certain partial differential equations, Numer Methods Partial Differential Equations 28 (2012), 506–522.
8. P. H. Wen and C. S. Chen, The method of particular solutions for solving scalar wave equations, Intl J Numer Methods Biomed Eng 26 (2010), 1878–1889.
9. A. R. Lamichhane and C. S. Chen, The closed-form particular solutions for Laplace and biharmonic operators using a Gaussian function, Appl Math Lett 46 (2015), 50–56.
10. A. S. Muleshkov, M. A. Golberg, and C. S. Chen, Particular solutions of Helmholtz-type operators using higher order polyharmonic splines, Comput Mech 24 (1999), 444–419.
11. G. M. Yao, Local radial basis function methods for solving partial differential equations, Ph.D. thesis, University of Southern Mississippi, Hattiesburg, MS, USA, 2010.
12. G. E. Fasshauer and J. G. Zhang, On choosing optimal shape parameters for RBF approximation, Numer Algorithms 45 (2007), 345–368.
13. C.-S. Huang, C. F. Lee, and A. H.-D. Cheng, Error estimate, optimal shape factor, and high precision computation of multiquadric collocation method, Eng Anal Bound Elem 31 (2007), 614–623.

14. E. J. Kansa, Multiquadric—a scattered data approximation scheme with applications to computational fluid-dynamics. 2. Solutions to parabolic, hyperbolic and elliptic partial-differential equations, Comput Math Appl 19 (1990), 147–161.

15. S. Rippa, An algorithm for selecting a good value for the parameter c in radial basis function interpolation, Adv Comput Mat 11 (1999), 193–210.

16. H. Y. Tian, S. Reutskiy, and C. S. Chen, A basis function for approximation and the solution of partial differential equations, Numer Partial Differential Equations 24 (2008), 1018–1036.

17. C. H. Tsai, J. Kolibal, and M,. Li, The golden section search algorithm for finding a good shape parameter for meshless collocation methods, Eng Anal Bound Elem 34 (2010), 738–746.

18. J. Wertz, E. J. Kansa, and L. Ling, The role of the multiquadric shape parameters in solving elliptic partial differential equations, Comput Math Appl 51 (2006), 1335–1348.

19. J. Duchon, Fonctions-spline du type plaque mince en dimension 2, Seminaire d'Analyse Numerique, Universite Scientifique et Medicale de Grenoble, 231, 1975.

20. J. Duchon, Fonctions-spline energy invariate par rotation, Technical Report 27, Math. Appl. Universite Scientifique et Medicale de Grenoble, 1976.

21. G. E. Fasshauer, Meshfree approximation methods with MATLAB, World Scientific, Illinois Institute of Technology, USA, 2007.

22. The Stanford 3D Scanning Repository, http://graphics.stanford.edu/data/3Dscanrep/, Accessed: 30 February 2017.

23. C. S. Chen, The method of fundamental solution for nonlinear thermal explosion, Commun Numer Methods Eng 11 (1995), 675–681.

24. A. A. Lacey, Mathematical analysis of thermal runaway for spatially inhomogenous reactions, SIAM J Appl Math 43 (1983), 1350–1366.

25. S. J. Hales and J. Levesley, Error Estimates for multilevel approximation using polyharmonic splines, Numer Algorithms 30 (2002), 1–10.

26. A. Iske, On the stability of polyharmonic spline reconstruction, In Conference Proceedings of Sampling Theory and Applications (SampTA2011), University of Hamburg, Germany.

27. C. A. Micchelli, Interpolation of scattered data: distance matrices and conditionally positive definite functions, Constr Approx 2 (1986), 11–22.